

Ultrafast Collective Dynamics in the Charge-Density-Wave Conductor $\text{K}_{0.3}\text{MoO}_3$

Yuhang Ren¹, Zhu'an Xu², and Gunter Lüpke¹

¹*Department of Applied Science, College of William and Mary,
Williamsburg, VA 23187*

²*Department of Physics, Zhejiang University, Hangzhou, Zhejiang 310027,
P. R. China*

(November 9, 2018)

Abstract

Low-energy coherent charge-density wave excitations are investigated in blue bronze ($\text{K}_{0.3}\text{MoO}_3$) and red bronze ($\text{K}_{0.33}\text{MoO}_3$) by femtosecond pump-probe spectroscopy. A linear gapless, acoustic-like dispersion relation is observed for the transverse phasons with a pronounced anisotropy in $\text{K}_{0.33}\text{MoO}_3$. The amplitude mode exhibits a weak (optic-like) dispersion relation with a frequency of 1.67 THz at 30 K. Our results show for the first time that the time-resolved optical technique provides momentum resolution of collective excitations in strongly correlated electron systems.

A charge-density wave (CDW) incorporates a periodic modulation of the crystal's valence charge and is usually accompanied by a small periodic lattice distortion [1,2]. The symmetry-breaking charge modulation lowers the energy of the occupied electronic states and raises that of the unoccupied states, opening up a band gap, so that the CDW state becomes stable below a certain critical temperature T_{CDW} [2]. Recent investigations of CDW conductors have been concerned with the low-energy collective excitations because of their dramatic dynamical responses, including loading and unloading cycles, plastic motion, and intermittent avalanches, which are directly related to the collective motion of magnetic flux quanta in high-temperature superconductors and charge-ordering fluctuations in colossal magnetoresistance manganites [3–8]. However, very few experimental results on collective mode spectra are available, especially in the low-energy region [3,4].

Ultrafast optical spectroscopy has provided important information on the intricate dynamics of collective modes and quasi-particles in metals [9–11], and more recently transition metal oxides [7,8,12,13]. The coherent excitation of an amplitude mode (amplitudon) has been observed by time-resolved transient reflectivity experiments in the quasi-one dimensional CDW conductor, $K_{0.3}MoO_3$, and the photo-generation mechanism has been described by displacive excitation of coherent phonons (DECP) [8]. However, to our knowledge the photo-induced excitation of the low-energy phase modes (phasons), which are acoustic-like and therefore govern the low-frequency CDW dynamics [3], have not yet been reported.

Here, we report on the first time- and momentum-resolved optical spectroscopy of collective CDW excitations in the quasi-one dimensional conductor, K_xMoO_3 (KMO) with $x = 0.3$ and 0.33 , in the long-wavelength limit below the CDW transition temperature, T_{CDW} . We present the dispersion relation and anisotropy of the transverse phase mode in KMO in the low-frequency range from $5 - 40$ GHz. The transverse phason exhibits an acoustic-like linear dispersion relation with a phase velocity of $c_0 = 2.4 \pm 0.3 \times 10^3$ m/s along the chain direction. In red bronze, $K_{0.33}MoO_3$, the phason oscillations reveal a pronounced anisotropy and vanish when the probe beam polarization is perpendicular to the chain direction. This strong anisotropy of $K_{0.33}MoO_3$ represents a clear signature of the

transverse phason and is explained by short-range correlations perpendicular to the chain direction. The amplitude mode exhibits a weak (optic-like) dispersion relation with a frequency $\Omega_+(q = 0) = 1.67$ THz at 30 K. Our results show that *the time-resolved optical technique provides momentum-resolved spectroscopic information* on the low-energy dynamics of collective excitations in strongly correlated electron systems. This important new information is relevant for the elucidation of collective transport phenomena in high- T_C superconductors and colossal magneto-resistance materials.

In the time-resolved optical experiments, a KMO single crystal is excited by 150-fs pump pulses at 1.55-eV photon energy delivered by a Ti:sapphire regenerative amplifier operating at 1-KHz repetition rate. The KMO single crystals (5 mm*5 mm*0.5 mm) are c -axis oriented. The probe beam, polarized parallel to the sample surface, probes directly the $(a' - b)$ -plane reflectivity, where a' represents the $[102]$ direction of the KMO single crystal. The b -axis is the direction along the chains. An optical parametric amplifier (OPA-800C, Spectra-Physics) provides the 150-fs probe pulses tunable in wavelength from 400 nm to 10 μm . The unfocused pump beam, spot-diameter 2 mm, and the time-delayed probe beam are overlapped on the sample with their polarization perpendicular to each other. The typical pump beam power is less than 4 mW, and the probe beam power is less than 1 mW. The change of the reflected probe beam intensity (ΔR) induced by the pump beam is recorded as a function of time delay for different wavelengths of the probe beam ($\lambda_{\text{probe}} = 400 \text{ nm} - 2.5 \mu\text{m}$). A SR250 gated integrator & boxcar averager, and a lock-in amplifier are used to measure the transient reflectivity change ΔR of the probe beam.

Figure 1 shows the time evolution of ΔR for a $\text{K}_{0.3}\text{MoO}_3$ single crystal at 35 K. The data are taken with pump and probe wavelength at 800 nm. The probe beam polarization is parallel to the chain direction ($E \parallel b$). The decay of ΔR shows two damped oscillatory components on top of a bi-exponential decay. The fast oscillations of ΔR are shown on a picosecond time scale in the inset of Fig. 1. The trace shows several damped oscillations. The frequency of these oscillations is ~ 1.67 THz obtained by Fourier transformation. This value is in good agreement with the frequency of the amplitude mode in $\text{K}_{0.3}\text{MoO}_3$ obtained from

previous time-resolved optical measurements [8], as well as neutron and Raman scattering [14,15]. The amplitude of the fast oscillation is independent of the probe pulse polarization and rather isotropic in the $a' - b$ plane, which is consistent with the A_1 symmetry of the amplitude mode. Besides the fast oscillations, the data also reveal a slow strongly overdamped modulation of ΔR (Fig. 1). The frequency of this mode is 0.015 THz.

In order to identify the nature of these slow oscillations we performed spectroscopic measurements of ΔR as a function of probe wavelength in the range from 400 to 2500 nm. Figure 2 shows the dispersion relations of the slow and fast oscillations of ΔR in $\text{K}_{0.3}\text{MoO}_3$ at 30 K. The wave number is given by $q = 2n/\lambda_{\text{probe}}$, where $n \simeq 3$ is the refractive index of $\text{K}_{0.3}\text{MoO}_3$ [16]. The dispersionless amplitude mode exhibits a gap for $q \rightarrow 0$, with a frequency $\Omega_+(q=0) = 1.67$ THz (Fig. 2). The frequency dependence of the slow oscillation shows clearly a linear, acoustic-like dispersion. The linear dispersion relation together with the very low frequency, $\nu = 5 - 40$ GHz and small phase velocity, $c_0 = 2.4 \pm 0.3 \times 10^3$ m/s, indicates the photo-excitation of a transverse phason [17]. The agreement is excellent between our experimental data and the transverse phase velocity normal to the surface, 23 ± 4 THzÅ, obtained by neutron inelastic scattering [18].

A clear signature of the transverse phason dynamics is obtained from the anisotropy and doping concentration dependence of period and amplitude of the low-frequency oscillations in KMO. Figure 3 shows the time evolution of ΔR for probe beam polarizations parallel ($E \parallel b$) and perpendicular ($E \perp b$) to the chain direction in $\text{K}_{0.3}\text{MoO}_3$ at 30 K (Fig. 3(a)) and $\text{K}_{0.33}\text{MoO}_3$ at 290 K (Fig. 3(b)). The data are taken with the pump laser wavelength at 800 nm, whereas the probe wavelength is 400 nm. The most striking result is the pronounced anisotropy of the coherent oscillations in red bronze (Fig. 3 (b)). A strong oscillatory signal occurs when the polarization of the probe beam is parallel to the chain direction, $E \parallel b$. The oscillations fade away in the direction of $E \perp b$. The amplitude of the transverse phason is expected to be strongly anisotropic in $\text{K}_{0.33}\text{MoO}_3$, since only short-range correlations occur along the chain direction. Coulomb interaction cannot lead to a coherent CDW modulation on neighboring chains [19] and therefore the coherent oscillations in ΔR disappear when the

probe polarization is perpendicular to the chain direction.

For the quasi-1D conductor $\text{K}_{0.3}\text{MoO}_3$, density wave fluctuations on neighboring chains become correlated because of interchain interactions. This leads to a transition to a ground state with three-dimensional, long-range order at $T_{CDW} = 183$ K. Coulomb interaction between neighboring chains tends to align the chains with a certain coherence length [20]. The coupling is different (anisotropic) parallel and perpendicular to the chain [20]. The anisotropy can be observed from the 400-nm data of $\text{K}_{0.3}\text{MoO}_3$ (Fig. 3(a), inset) [21]. As the probe beam polarization is rotated from parallel to perpendicular to the chain direction, the modulation period changes from 23.5 ps ($E \parallel b$) to 33 ps ($E \perp b$).

Since the optical properties in the two bronzes are very similar at photon energies in the near infrared to visible range [19], the stronger damping observed in $\text{K}_{0.3}\text{MoO}_3$ must be related to the damping of the transverse phason. The oscillations in $\text{K}_{0.33}\text{MoO}_3$ persist for at least 600 ps with very little damping, whereas $\text{K}_{0.3}\text{MoO}_3$ exhibits only five periods of the oscillation (Fig. 3). A least-square fit of the 400-nm data in $\text{K}_{0.3}\text{MoO}_3$ gives a damping constant $\tau_p \simeq 60$ ps for the transverse phason oscillation at $\Omega_- = 0.035$ THz (Fig. 3 (a)). This value is quite different from the fast damping time, $\tau_A \simeq 10$ ps, observed for the amplitude mode [14] and is larger than the values reported for the phason from far-infrared [22] and neutron scattering measurements [15]. However, the damping constant is in good agreement with the underdamped response from ac-conductivity measurements [23]. The difference may be explained by the coupling between pinned modes and transverse phasons in distinct frequency ranges.

Next, we present a simple physical model that accounts correctly for our observations. In our experiments, the number of photons per pulse and unit volume absorbed in the sample is $\sim 10^{20}$ photons/cm³, comparable to the charge-carrier density ($\sim 10^{20}$ - 10^{21} holes/cm³) in KMO; hence, one expects significant electron excitation during ultrashort pump pulse illumination. This generates coherent collective modes: amplitudon and phason. This excitation mechanism is clearly different from previous pump-probe transmission experiments in weakly absorbing materials [24,25]. In the latter case the wave-vector of the excited modes

is determined by the phase-matching condition of the pump beam, whereas in our case the frequencies of the collective modes are independent of the polarization and wavelength of the pump beam. Since the penetration depth, ξ , in KMO is very small (~ 100 nm), impulsive excitation of the solid on a time scale shorter than the material's hydrodynamic response time generates a broad spectrum of collective modes down to frequencies of order $c_0/\xi \sim 5$ GHz [26].

We use a tunable optical probe pulse to detect the various frequency components of the photo-generated collective modes. In the back-scattering geometry (Fig. 4), part of the probe pulse is reflected by the wave front of the excited CDW modes, and the remainder at the surface of the KMO crystal. These reflections interfere constructively or destructively depending on the position and time of the charge density modulation. Further, the momentum selection rule for back scattering is $q_i + q_f = q \cos \theta$, where q_i and q_f are the wave vectors of the incident and scattered probe beam in the material, and θ is the probe beam incident angle ($\theta \sim 0^\circ$). Therefore, for a given probe wavelength phase-matching occurs exclusively on a single wave vector of the collective excitation. This process causes the probe signal to oscillate with time delay relative to the pump pulse.

In principle, both the longitudinal and transverse phason should couple to the probe pulse and induce coherent oscillations in the time-resolved reflectivity change, ΔR . However, since the pump spot size at the sample is quite large, the surface area within that spot is excited in a more or less spatially uniform manner. The pump pulse is strongly absorbed at the surface, so that the photo-excitation has a large gradient going into the sample from the surface, and a very small gradient across the pump spot. The wave vector component must be very nearly zero in any direction along the surface (also along the chain direction) but can be large in the direction normal to the surface (i.e. transverse to the chain direction). This is similar to ultrafast excitation of acoustic wavepackets that propagate into the sample from a strongly absorbing material [27,28]. Thus, the charge density wave propagation develops in KMO normal to the surface, i.e., $(a' - b)$ plane, so that only the transverse phason is generated. The novelty of this experiment is that *the time-resolved optical technique can be*

used in a momentum-resolved way.

Finally, we would like to mention possible applications of our results. The manipulation of amplitude, phase and momentum of a charge density wave using ultrafast laser pulses represents an approach similar to coherent control of optical phonons performed on GaAs and GaAs/AlAs superlattices, Bi films, and crystalline quartz [28]. The phason and amplitudon can be set and detected to a high degree of accuracy. In effect, the collective mode excitation can be used as a switchable THz optical modulator whose amplitude and phase can be controlled by ultrashort laser pulses. The potential advantages of our variant are the magnitude of the effect, frequency tunability, perpendicular propagation, and large lateral dimensions.

We thank Profs. Serguei Artemenko and Keith Nelson for valuable comments and discussions. This work is supported in part by NSF-DMR-0137322 (CWM) and the National Natural Science Foundation of China (Grant no. 10225417).

REFERENCES

- [1] See, e.g., *Electronic Properties of Inorganic Quasi-One-Dimensional Compounds*, Ed. by P. Monceau, (Reidel Publ. Co., 1985).
- [2] See, e.g., *Charge Density Waves in Solids*, Ed. by L. P. Gor'kov and G. Gruner, (North Holland, Amsterdam, 1989); *Density Waves in Solids*, Ed. by G. Grüner, (Addison-Wesley, Reading, MA, 1994).
- [3] See, e.g. *Proceedings of the International Workshop on Electronic Crystals*, 1999, Ed. by S. Brazovskii, P. Monceau, *J. Phys. France IV*, 9 1999; *Proceedings of the International Workshop on Electronic Crystals*, 2002, Ed. by S. Brazovskii, N. Kirova and P. Monceau, *J. Phys. France IV*, 12, 2002.
- [4] J. Dumas and C. Schlenker, *Int. Journ. Mod. Phys.* 7, 4045 (1993).
- [5] Y. -D. Chuang, A. D. Gromko, D. S. Dessau, T. Kimura, and Y. Tokura, *Science* 292, 1509 (2001).
- [6] N. Kida and M. Tonouchi, *Phys. Rev. B* 66, 024401 (2002).
- [7] R. A. Kaindl, M. Woerner, T. Elsaesser, D. C. Smith, J. F. Ryan, G. A. Farnan, M. P. McCurry, and D. G. Walmsley, *Science* 287, 470 (2000).
- [8] J. Demsar, K. Biljakovic, and D. Mihailovic, *Phys. Rev. Lett.* 83, 800 (1999).
- [9] G. L. Eesley, *Phys. Rev. Lett.* 51, 2140 (1983).
- [10] E. Beaurepaire, J.-C. Merle, A. Daunois, and J.-Y. Bigot, *Phys. Rev. Lett.* 76, 4250 (1983).
- [11] B. Koopmans, M. van Kampen, J. T. Kohlhepp, and W. J. M. de Jonge, *Phys. Rev. Lett.* 85, 844 (2000).
- [12] J. S. Dodge, A. B. Schumacher, J.-Y. Bigot, D. S. Chemla, N. Ingle and M. R. Beasley, *Phys. Rev. Lett.* 83, 4650 (1999).

- [13] T. Kise, T. Ogasawara, M. Ashida, Y. Tomioka, Y. Tokura, and M. Kuwata-Gonokami, Phys. Rev. Lett. 85, 1986 (2000).
- [14] G. Travaglini, I. Morke and P. Wachter, Sol. State. Commun. 45, 289 (1983).
- [15] J. P. Pouget, B. Hennion, C. Escribe-Filippini, and M. Sato, Phys. Rev. B 43, 8421 (1991).
- [16] B. P. Gorshunov, A. A. Volkov, G. V. Kozlov, L. Degiorgi, A. Blank, T. Csiba, M. Dressel, Y. Kim, A. Schwartz, and G. Grüner, Phys. Rev. Lett. 73, 308 (1994).
- [17] We can exclude the explanation of the photo-excitation of coherent longitudinal acoustic phonons (CLAPs) from the anisotropy of the coherent oscillations (Fig. 3). For KMO, the reflectivity [19] and the optical conductivity [16] is isotropic for wavelengths in the visible range, i.e. photon energy >2 eV. Therefore, photoexcitation of CLAPs would result in polarization-independent (isotropic) oscillations of ΔR at 400-nm probe wavelength.
- [18] B. Hennion, J. P. Pouget, M. Sato, Phys. Rev. Lett. 68, 2374 (1992). A factor of 2π is missing in the calculation of the phason velocity which had been included in ref. [15].
- [19] G. Travaglini, P. Wachter, J. Marcus, and C. Schlenker, Sol. State. Comm. 37, 599 (1981); 42, 407 (1982).
- [20] S. Girault, A. H. Moudden, J. P. Pouget, Phys. Rev. B 39, 4430 (1989).
- [21] The anisotropy can not be explained by the optical properties of $K_{0.3}MoO_3$ since the reflectivity and optical conductivity is isotropic at photon energies above 2 eV [16,19].
- [22] H. K. Ng, G. A. Thomas, and L. F. Schneemeyer, Phys. Rev. B 33, 8755 (1986).
- [23] G. Mihaly, Phys. Scr. 29, 67(1989); G. Mihaly, T. W. Kim, and G. Grüner, Phys. Rev. B 39, R13009 (1989).
- [24] T. E. Stevens, J. K. Wahlstrand, J. Kuhl, and R. Merlin, Science 291, 627 (2001).

- [25] R. M. Koehl and K. A. Nelson, J. Chem. Phys. 114, 1443 (2001).
- [26] O. B. Wright, J. Appl. Phys. 71, 1617 (1992).
- [27] C. Thomsen, H. T. Grahn, H. J. Maris, and J. Tauc, Phys. Rev. B 34, 4129 (1986).
- [28] H. -Y. Hao and H. J. Maris, Phys. Rev. Lett. 84, 5556 (2000); Phys. Rev. B 63, 224301 (2001).

Figure Captions:

Fig. 1 Reflectivity change ΔR at 800-nm probe wavelength from $\text{K}_{0.3}\text{MoO}_3$ single crystal at 35 K. The inset depicts the fast oscillations on a short time scale.

Fig. 2 Phason (Ω_-) and amplitudon (Ω_+) dispersion relations of $\text{K}_{0.3}\text{MoO}_3$ at 30 K.

Fig. 3 Transient reflectivity change ΔR at 400-nm probe wavelength: a) with the polarization vector E parallel ($E \parallel b$) and perpendicular ($E \perp b$) to the chain direction in $\text{K}_{0.3}\text{MoO}_3$. The inset shows the anisotropy of the oscillation period in the $a' - b$ plane. b) Anisotropy of ΔR for different probe polarization angles in the $a' - b$ plane of $\text{K}_{0.33}\text{MoO}_3$.

Fig. 4 Illustration of the photo-induced transverse phason excitation and detection mechanism. For details see text.

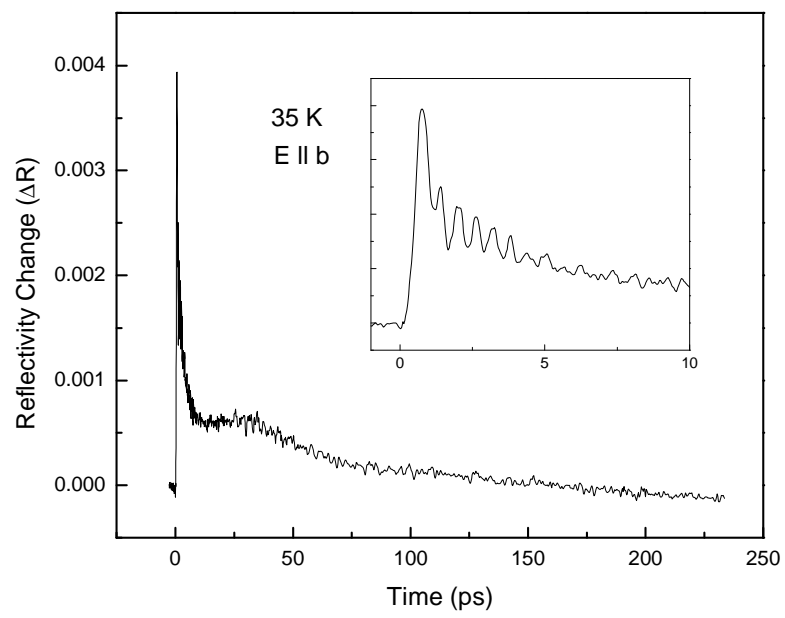


Fig. 1

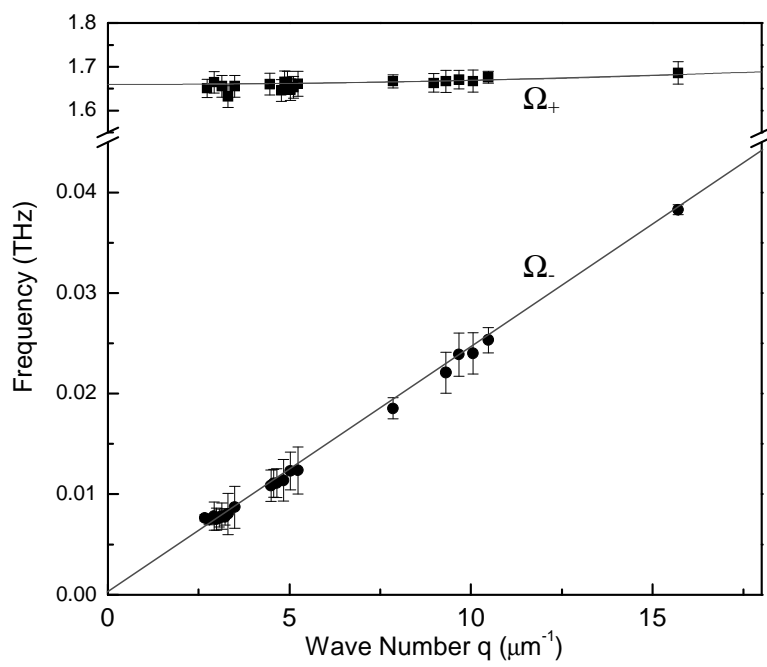


Fig. 2

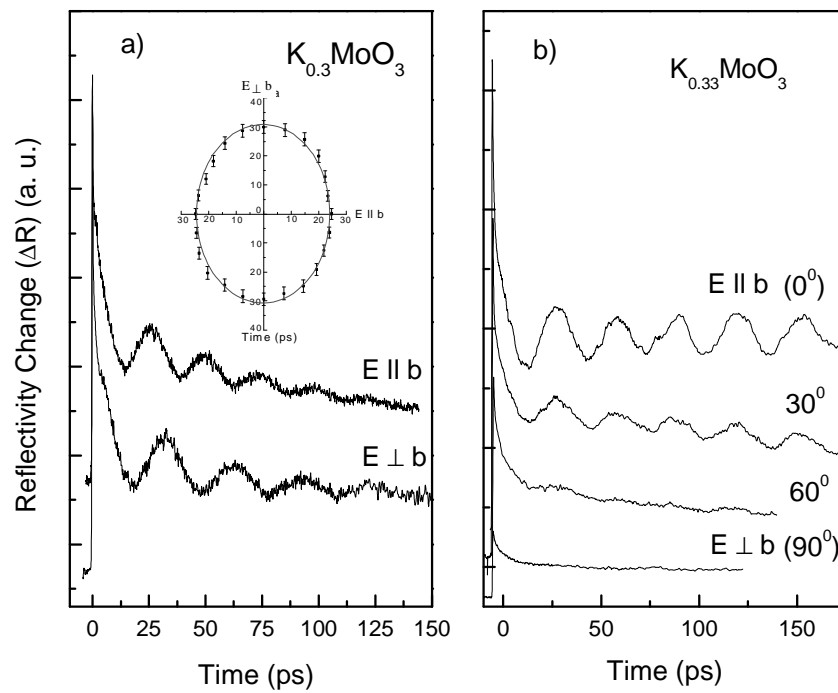


Fig. 3

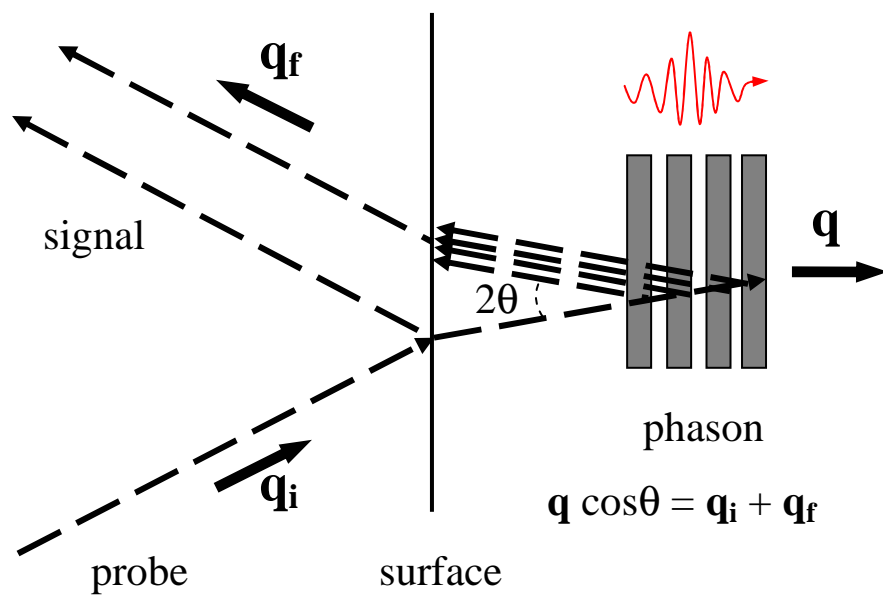


Fig. 4